Test of Approximations to Surface Motion in Gas−Surface Dynamics: Linear versus Quadratic Coupling for $T_s = 0$ K†

Z. S. Wang,‡,§ G. R. Darling,‡ B. Jackson,|| and S. Holloway*,‡

Surface Science Research Centre, Department of Chemistry, University of Liverpool, L69 3BX, U.K. and Department of Chemistry, University of Massachusetts, Amherst, Massachusetts 01003

Received: April 11, 2002; In Final Form: June 10, 2002

A coupled wave vector formalism is applied to compute the reduced density matrix for dissociation and inelastic scattering of D_2 molecules on Cu surfaces at finite temperature. The effect of lattice recoil at 0 K is utilized to test different levels of approximation to the molecule-lattice coupling in the Hamiltonian. Although the first order, linear coupling term is found adequate to account for the surface recoil effect in D_2 scattering with rotational transitions, the quadratic term is required for an adequate description of the recoil accompanying dissociation, a process characterized by a stronger interaction between the incident molecule and the activation barrier present in the D_2/Cu potential energy surface (PES). A detailed analysis is carried out using a low-dimensional model PES, changing the location of the dissociation barrier. This reveals that the necessity of the quadratic term for dissociation can be attributed to a late barrier. For an early barrier, in the entrance channel, the linear coupling approximation is sufficient to describe dissociation.

1. Introduction

The influence of thermal lattice motion on molecular dissociation on and inelastic scattering from metal surfaces is an issue important for a very broad range of scientific and technological fields.[1,2] Significant developments have been made in recent years both in experiment and in theory and have provided valuable insights into the surface temperature dependence of various molecular processes. Deployment of up-to-date molecular beam techniques, such as stimulated Raman pumping of the initial molecular state, has enabled measurement at the state-to-state level.[3,4] On the theory side, steady improvement in the computation of the potential energy surface (PES)[5] has been accompanied by a concomitant increase in the power of quantum wave packet dynamics methods.[6,7] Hydrogen dissociation on metal surfaces, which has served as a benchmark system for gas−surface reaction dynamics,[8] continues to be the focus of many finite-temperature studies.[9−12] For hydrogen on transition metals, simple two-body energy transfer is small because of the mismatch in mass between the hydrogen molecule and surface atoms. Therefore, it is quite surprising that recent experiments have shown that for the H_2/Cu[9,12] and H_2/Pd[10,11] systems the surface temperature dependence of several processes is well described by an Arrhenius law. This is remarkable because the systems differ from each other dramatically in the underlying PES: the H_2/Pd PES possesses molecular chemisorption wells that can possibly lead to trapping and equilibration with the substrate [13−18] in addition to steering,[13,14,19] whereas H_2/Cu is the archetypal activated direct scattering/dissociation system unable to support any trapping and thermal equilibrium with the surface. The puzzle has been solved to a certain extent by high-dimensional dynamics models,[7,17] which reproduced the trend in the experimental data.

Despite great progress already made, high-dimensional, quantum dynamics calculations involving the thermal substrate motion remain a challenge because of their heavy requirements for computational resources. A general method to treat the molecule−heat-bath system is the density matrix (DM) formalism. An economic way of doing DM calculations is to work with the reduced density matrix for the molecule, which is obtained by tracing over the bath states. Despite some low-dimensional implementations in gas−surface dynamics,[20−24] the DM method is formidable in practice for more than two dimensions. An alternative way of performing thermally dependent quantum dynamics computations for molecules on metals is based on the idea of treating the lattice motion with a single oscillator that rigidly shifts the static surface PES and thereby couples to the incident molecule. The single oscillator approximation was introduced more than thirty years ago[25,26] to deal with rare gas scattering from metal surfaces, and many calculations adopting this approximation have afforded excellent agreement with experimental data. Propagating the wave packet for the molecule−oscillator system starting from an individual phonon state leads to phonon-state specific cross sections for molecular dissociation and scattering. Direct Boltzmann averaging then yields all of the temperature-dependent cross sections. This strategy, although clearly a simplification, has enabled quantum dynamics calculations on realistic, high-dimensional PESs, and the results have been found to be in good agreement with experimental data.[7,27−29] Recently, Jackson[30] has demonstrated that for this single oscillator model the evolution of the reduced density matrix can be described by a set of coupled wave vectors. In a two (molecular) degree-of-freedom study of H_2 dissociation, he demonstrated that this could lead to a tremendous saving of memory and computational effort. However, to implement this model, the full molecule plus oscillator potential must be expanded in powers of the oscillator

† Part of the special issue "John C. Tully Festschrift".

* To whom correspondence should be addressed.

‡ University of Liverpool.

§ Present address: Department of Chemistry and Biochemistry, University of Texas at Austin, TX 78713. E-mail: zswang@mail.cm.utexas.edu.

|| University of Massachusetts.

10.1021/jp020938+ CCC: $22.00
Published on Web 07/16/2002

displacement, and Jackson considered only the first (linear) term. In fact, most theoretical descriptions of molecules coupled to heat baths are based upon such expansions. In nearly all cases, these expansions are truncated at the linear term, assuming that at typical temperatures the thermal displacements of the bath particles from their equilibrium positions are relatively small. Whether higher order terms are needed is an important and relatively unexplored question which we consider in this work.

In the present paper, we shall extend the coupled wave vector (CWV) method of Jackson to high dimensionality to study molecular dissociation on and scattering from metal surfaces at finite temperature. Nowhere in this present paper will we consider the important process of nonadiabaticity induced by electron−hole pair excitation. This does not mean that we believe this to be an insignificant channel for inelastic processes, and indeed, this has been considered elsewhere.[31] Here, we shall examine the performance of the approximations for truncating the Hamiltonian for phonon excitation only. This will be done for the hydrogen/Cu system as an example. We shall utilize the lattice recoil phenomenon as a platform to assess the sufficiency of the approximations. The recoil is a measure of the energy loss from the molecule to the lattice at temperatures close to absolute zero and thus is a theoretical prediction subject to experimental test.[32] Comparing the recoil predicted by the CWV method to that from direct Boltzmann averaging based on wave packet dynamics enables an assessment of the quality of the approximations. On the basis of the findings from the high-dimensional calculations, a low-dimensional analysis will be conducted to identify the essential topographical properties of the underlying PES responsible for the success or failure of the approximations.

The remaining part of the paper is organized in four sections. In section 2, we shall outline the theories used in the present study and the PES. In the next section, we shall present results from the high-dimensional dynamics calculations for D_2 dissociation and scattering on Cu(111). Section 4 is a two-dimensional analysis to identify topological characters of the PES that are responsible for the performance of the approximations. We draw conclusions in section 5.

2. Theoretical Formalism

2.1. Hamiltonian in the Single Oscillator Approximation. The basic idea of the single oscillator approximation is to divide the lattice into a primary region, which interacts strongly with the molecule and can be approximated as a single surface atom attached to a harmonic restoring force, and a secondary region that is the remainder of the substrate, which serves as a heat bath.[25,26] Thus, we deal with an independent, localized Einstein oscillator. Because studies on rare gas scattering[33] have shown that the lattice recoil normal to the surface plane dominates inelastic behavior, the oscillator is confined to this dimension. The oscillator is assigned the mass of a surface atom, M_s, and a frequency given by the surface Debye frequency, ω_s. It is assumed that the ensemble of such oscillators is in equilibrium with surface temperature T_s. Thus, the temperature dependence can be incorporated by initializing the oscillator with different states and averaging over the final results according to a Boltzmann distribution. Although lacking a firm foundation from first principles, the single oscillator approximation has proved successful in practice. Dissipation of the energy of the oscillator into the secondary region of the lattice is usually neglected, because the molecule−surface interaction occurs within a time scale shorter than that of the substrate relaxation.[34,35]

In this paper, we deal with a normally incident diatomic molecule at a single surface site. In addition to the surface oscillator coordinate, y, four molecular degrees of freedom were treated explicitly: the distance between the molecular center of mass and the surface, Z, the molecular bond length, r, and the bond orientation (θ,ϕ) relative to the surface normal. Following previous single oscillator studies,[29,32] we assume that the surface oscillator couples to the incident molecule via translational motion. Thus, the potential energy for the molecule-oscillator system is $V(Z-y,r,\theta,\phi)$, where $V(Z,r,\theta,\phi)$ is the PES for the static surface. This scheme ignores any possible distortion of the PES caused by changes of the local atomic geometry from the ideal surface upon impact. The magnitude of this effect is still in debate.[30,36]

The Hamiltonian for the diatomic−surface oscillator system then reads as

$$H = T_m + T_{osc} + \frac{1}{2}M_s\omega_s^2 y^2 + V(Z-y,r,\theta,\phi) \qquad (1)$$

where the kinetic operators for the molecule and oscillator are (using atomic units throughout)

$$T_m = -\frac{1}{2M}\frac{\partial^2}{\partial Z^2} - \frac{1}{2\mu}\frac{\partial^2}{\partial r^2} - \frac{1}{2\mu r^2}L^2 \qquad (2)$$

$$T_{osc} = -\frac{1}{2M_s}\frac{\partial^2}{\partial y^2} \qquad (3)$$

Here M and μ are the total and reduced mass of the diatomic.

2.2. Solution to the Dynamics: Direct Wave Packet Propagation. Within the single oscillator approximation, the surface temperature-dependent dynamics can be solved by propagating the total wave packet for the molecule plus oscillator system, $\Psi(Z,r,\theta,\phi,y;t)$, for different initial phonon states. [We shall use phonon state to refer to the state of the single oscillator for consistency with the more general problem of scattering from a surface in thermal motion.] Surface temperature dependent cross sections can be obtained by Boltzmann averaging the final results over many phonon states. This strategy is straightforward, enables fully quantum-mechanical treatment of the dynamics, but is computationally demanding because the wave packet calculation has to be repeated for many states to ensure convergence.

Expanding the total wave function, $\Psi(Z,r,\theta,\phi,y,t)$, in terms of the oscillator eigenfunctions, $\Phi_n(y)$, and applying the Hamiltonian, one obtains the time-dependent Schrödinger equation

$$i\frac{\partial\Psi_n(Z,r,\theta,\phi;t)}{\partial t} = \left[T_m + \left(n+\frac{1}{2}\omega_s\right)\right]\Psi_n + \sum_m \Psi_m\langle\Phi_n|V(Z,r,\theta,\phi,y)|\Phi_m\rangle \qquad (4)$$

Representing Ψ_n on a finite-element grid in the molecular coordinates, we have solved the Schrödinger equation with the split-operator method.[37] The diagonal kinetic energy operators were computed with a highly efficient, symmetry-adapted discrete variable representation,[38] whereas the nondiagonal potential operator was treated using a Chebychev expansion.[39] The phonon expansion included nine channels centered on the initial phonon state; this was sufficient for convergence. To obtain the cross section at $T_s = 0$ K, one needs to propagate the wave packet for only a single, initial phonon state, namely,

the ground-state harmonic function. This simplifies the present calculations of surface recoil. Details of the wave packet model and its predictions for finite-temperature cross sections can be found in ref 40.

2.3. Solution to the Dynamics: Reduced Density Matrix Computed via a Coupled Wave Vector Formalism. The general method to solve the dynamics of a molecular system coupled to a heat bath is density matrix formalism. The appropriate (thermal) density matrix for the molecule-oscillator system is

$$\rho = \sum_n \frac{1}{Z} e^{-E_n/k_B T} |\Psi_n(t)\rangle\langle\Psi_n(t)| \quad (5)$$

where E_n is the eigenenergy for nth phonon state. The equation of motion for ρ is

$$\frac{\partial \rho}{\partial t} = -i[H,\rho] \quad (6)$$

Tracing over all bath states leads to the reduced density matrix for the molecule, $\sigma = \mathrm{tr}_b\, \rho$. Unfortunately, there is no exact equation of motion for the reduced density matrix σ. The density matrix method has been applied in gas−surface dynamical studies using empirical models for the dissipation.[22,23] These studies are computationally demanding because one has to deal with evolution of a full matrix. If the molecule-bath coupling is defined using the single oscillator approximation, then it is possible to solve for the reduced density matrix with a set of wave vectors instead of a full matrix. Here, we briefly outline the wave vector formalism introduced by Jackson.[30]

The full molecule-bath wave function can be rewritten as

$$\Psi_n(Z,r,\theta,\phi,y;t) = \sum_{\alpha=-\infty}^{\infty}\sum_{s=0}^{\infty}\Psi_{\alpha s}(Z,r,\theta,\phi;t)\, A_\alpha (a^+ a)^s e^{-iE_n t}\, \Phi_n(y) \quad (7)$$

where a^+ and a are the creation and annihilation operators for phonons, which satisfy the relation $y = (^1/_2 M\omega_s)^{1/2}(a + a^\dagger)$. The operator $A_\alpha = a^{|\alpha|}$ for $\alpha \le 0$ and $A_\alpha = (a^\dagger)^\alpha$ for $\alpha > 0$. Here, α describes the molecule-bath energy transfer $\Delta E = \alpha\omega_s$, and s is a number for organizing perturbation order $2s + |\alpha|$. Inserting eq 7 into eqs 5 and 6 and tracing over the bath leads to coupled equations of motion for the molecular wave function $\Psi_{\alpha s}$:

$$\sum_{s'=0}^{\infty}\frac{\partial}{\partial t}\Psi_{\alpha s'}(Z,r,\theta,\phi;t)M_{ss'}^{(\alpha)} = -i\sum_{s'=0}^{\infty}[T_m + V(Z,r,\theta,\phi) + \alpha\omega_s]\Psi_{\alpha s'}(Z,r,\theta,\phi;t)M_{ss'}^{(\alpha)} - i\sum_{\alpha'}\sum_{s'=0}^{\infty}\langle (a^+ a)^s A_\alpha {}^+ [\sum_{k=1}^{\infty} V^{(k)}(Z,r,\theta,\phi)\,(a^+ + a)^k] A_{\alpha'} (a^+ a)^{s'}\rangle \Psi_{\alpha' s'}(Z,r,\theta,\phi;t) \quad (8)$$

where $M_{ss'}^{(\alpha)}(T_s) = \langle (a^\dagger a)^s A_\alpha^\dagger A_\alpha (a^\dagger a)^{s'}\rangle$ and the brackets represents a thermal average over the bath. Here we already applied an expansion of the molecule-bath coupling in terms of the oscillator coordinate y: $V(Z - y,r,\theta,\phi) = V(Z,r,\theta,\phi) + \sum_{k=1}^{\infty} V^{(k)}(Z,r,\theta,\phi)y^k$. Truncating the expansion to certain k orders, one can work out the final equation of motion:

$$\frac{\partial}{\partial t}\Psi_{\alpha s}(Z,r,\theta,\phi;t) = -i[T_m + V(Z,r,\theta,\phi) + \alpha\omega_s]\Psi_{\alpha s}(Z,r,\theta,\phi;t) - i\sqrt{1/(2M\omega_s)}V^{(1)}\sum_{s'=0}^{N_s}[g_{ss'}^{(\alpha^{1+})}\Psi_{\alpha+1,s'}(Z,r,\theta,\phi;t) + g_{ss'}^{(\alpha^{1-})}\Psi_{\alpha-1,s'}(Z,r,\theta,\phi;t)] - i(\sqrt{1/(2M\omega_s)})^2 V^{(2)}\sum_{s'=0}^{N_s}\begin{bmatrix} g_{ss'}^{(\alpha^{2+})}\Psi_{\alpha+2,s'}(Z,r,\theta,\phi;t) + g_{ss'}^{(\alpha^{2})}\Psi_{\alpha,s'}(Z,r,\theta,\phi;t) \\ + g_{ss'}^{(\alpha^{2-})}\Psi_{\alpha-2,s'}(Z,r,\theta,\phi;t) \end{bmatrix} \quad (9)$$

where the sum over s is limited to N_s terms in practice. The coupling coefficients are temperature dependent and can be worked out analytically:

$$g_{ss'}^{(\alpha+)} = \begin{cases} [(M^{(\alpha)})^{-1}M^{(\alpha+1)}]_{ss'} & \alpha \ge 0 \\ \delta_{ss'} & \alpha < 0 \end{cases}$$

At $T_s = 0$ K only g_{00}^{α} can be nonzero, all other couplings vanish. This will greatly simplify calculations of the recoil at 0K using the wave vector formalism.

If only the $k = 1$ terms are retained in eq 9, we have first order coupling and essentially deal with the linear coupling approximation. Then, Ψ_α is allowed to couple merely to $\Psi_{\alpha\pm1}$. We can go to the second order, quadratic coupling by truncating at $k = 2$, where Ψ_α can also be coupled to $\Psi_{\alpha+2}$ and $\Psi_{\alpha-2}$.

The structure of eq 9 is similar to eq 4 and will be solved using the same numerical procedure as applied to eq 4. Thus, the off-diagonal elements of the Hamiltonian matrix on the $\{\alpha,s\}$ basis are treated with Chebychev expansion to guarantee high-level accuracy in integrating eq 9.

The computational reduction achieved by this coupled wave vector method as compared to the conventional reduced density matrix method comes from the fact that there exist only a few nonzero off-diagonal elements if the linear (or quadratic) coupling approximation applies. Therefore, an important issue about the wave vector formalism is to assess the sufficiency of these approximations. The reduced density matrix is reconstructed from the wave vectors:

$$\sigma = \sum_s\sum_{s'}\sum_\alpha \Psi_{\alpha s}^*(Z,r,\theta,\phi;t)\Psi_{\alpha s'}(Z',r',\theta',\phi';t)M_{ss'}^{(\alpha)}(T_s) \quad (10)$$

All thermally averaged molecular properties can be obtained by tracing σ:

$$\langle O_m\rangle = tr_m O_m \sigma = \sum_n \frac{1}{Z} e^{-E_n/k_B T_s}\langle\Psi_n|O_m|\Psi_n\rangle \quad (11)$$

where O_m can be any molecular operator. The wave packet strategy described in section 2.2 corresponds to conducting the average straightforwardly.

2.4. Potential Energy Surface. A previously used model form with parameters appropriate for hydrogen/Cu(111) was used for the molecule-surface PES.[38] This PES is shown in Figure 1 for the broadside approach with the molecular bond parallel to the surface. It is characterized by a sharp elbow with a dissociation barrier located behind the corner of the elbow. The height of the barrier is about 700 meV. This late barrier allows for considerable extension of the molecular bond before dissociation and enables significant energy transfer from molecular translational to vibrational motion. The PES also includes

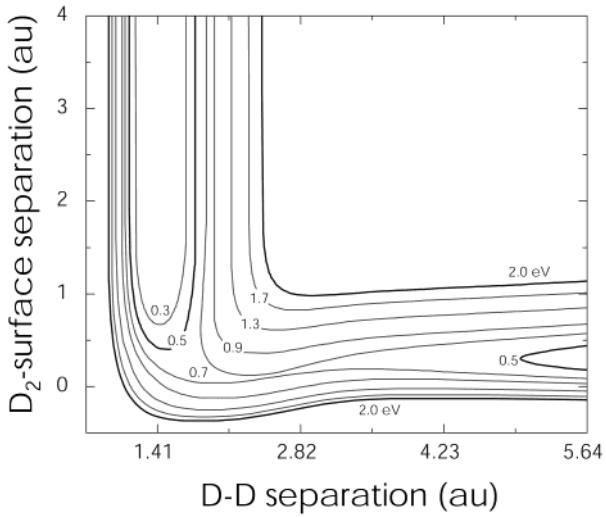

Figure 1. Potential energy surface for a D_2 molecule approaching Cu(111) in the broadside orientation, $\theta = \pi/2$. The PES has a dissociation barrier of 0.7 eV which is located toward the exit channel.

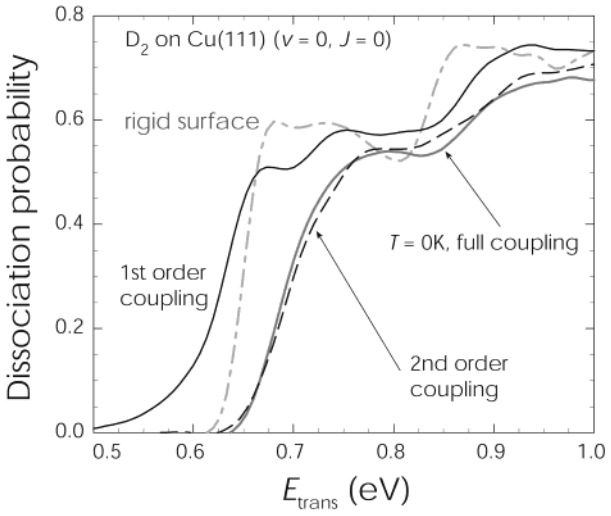

Figure 2. Probability for the dissociation of ($v = 0$, $J = 0$) D_2 on Cu(111) as a function of initial translational energy. The light gray dot−dashed line is the result of a molecular wave packet impinging on a rigid surface, whereas the solid gray line indicates results from similar calculations for a surface at 0 K which includes recoil. The 0 K results using the coupled wave vector method are also shown; the solid black line is from the linear coupling approximation, and the dashed line, the quadratic coupling approximation.

corrugation in the polar angle, θ of the D−D bond (not shown in the figure). The θ dependence favors in energy the approach of a flat-lying molecule over the head-on approach, thus facilitating translation-to-rotational energy transfer.[41] The dependence on the azimuthal angle ϕ is neglected, this is in line with a weak azimuthal dependence of the PES at atop sites of Cu.[42] For more details of the PES, readers are referred to ref 38. We have assigned the Einstein oscillator the mass of one Cu atom and a frequency equal to the surface Debye frequency of Cu(111) (14 meV).

3. Dissociation and Scattering Probabilities

In the present paper, we use the surface recoil at zero temperature as a platform to examine the linear or quadratic coupling approximation in the context of molecules dissociating on and scattering from metal surfaces. The recoil can be quantified by comparing cross-sections obtained from wave packet propagation with the surface oscillator included (initially in its ground state) to wave packet calculations for a rigid surface. The wave packet results can be regarded as the exact solutions for the recoil dynamics as far as the single oscillator approximation applies. Comparing the wave packet (WP) results to those of the coupled wave vector (CWV) formalism leads to a rigorous assessment of the approximations to the molecule-bath coupling. Hereafter, we shall present the results from WP and CWV computations for dissociation and for inelastic scattering of D_2 from Cu(111). All results are for zero surface temperature.

In Figure 2, we show the probability for dissociation of D_2 initially in the vibrational and rotational ground state ($v = 0$, $J = 0$) as a function of translational energy (E_{trans}). Several interesting features can be found in the figure. First, the clear evidence of recoil can be seen from the sizable shift of the WP result toward higher energy compared to the rigid surface result. The threshold change caused by introducing surface motion is about 25 meV. Recoil effects in dissociation of similar magnitude have been shown previously in lower-dimensional wave packet dynamics studies.[32,36,43] In a classical mechanics picture, the recoil can be qualitatively illustrated by a collision between a D_2 molecule and an unconstrained, moving barrier of height V^* with the mass of a Cu atom. Unlike a frozen lattice or a barrier of infinite mass, the relative motion then involves the reduced mass and therefore an effective barrier $V_{eff} = ((M + M_s)/M_s)\ V^*$.[32] Assigning V^* a value of 700 meV (the dissociation barrier of our D_2/Cu PES) yields a V_{eff} about 22.5 meV higher than the static barrier. This qualitatively accounts for the observed threshold increase due to the recoil. Recoil can therefore be thought of as a process where the molecule chases the barrier, to which it continuously loses energy. In addition to the threshold change, the rise of the dissociation probability also exhibits some differences: the rigid surface probability quickly reaches its saturation value about 60 meV above the threshold, whereas saturation is achieved in the case of the moving surface about 125 meV above the threshold. This broadening of the width of the dissociation curve can be attributed to the smearing of the threshold behavior due to the barrier recoil. Similar behavior has also been seen in previous lower-dimensional studies.

The CWV results for the dissociation probability obtained with first and second order coupling are also shown in Figure 2. We can see that when only the linear coupling term is included, the dissociation threshold is shifted to 125 meV *below* that of the exact WP calculation. In fact, the threshold is even shifted below that of the rigid surface; that is, there is no lattice recoil to first order. This situation is almost entirely remedied by including the second-order coupling, permitting two-phonon exchanges. Now the thresold is within 10 meV of the exact value. Indeed the overall E_{trans} dependence is very close to that of the exact result. These findings suggest that the energy transfer between the molecule and the surface is seriously misrepresented by the linear coupling approximation and that at least the quadratic coupling is required. However, we shall show below that these conclusions are not general but are actually dependent on the process being monitored (e.g., dissociation) and the topography of the region(s) of the PES explored by molecules undergoing this process.

As a further test of the CWV computations, we have also performed WP calculations using a Hamiltonian truncated to second order coupling. The dissociation probability thus obtained is almost identical to that for the CWV shown in Figure 2, with only very minor disagreements at the highest energies considered.

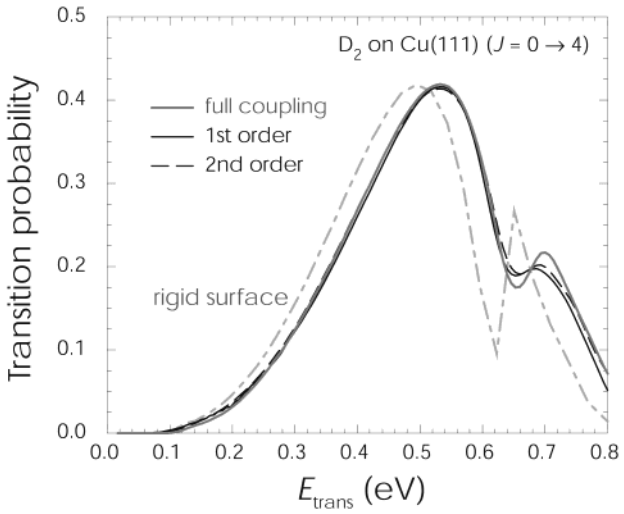

Figure 3. As Figure 2 but for the inelastic probability for scattering of D_2 from Cu(111) with rotational transition ($v = 0$, $J = 0 \rightarrow 4$).

The probability of rotational excitation ($v = 0$, $J = 0 \rightarrow 4$) of D_2 scattering from Cu(111) is presented in Figure 3 as a function of E_{trans}. The recoil is clearly visible but to a lesser extent than for dissociation (Figure 2). The smaller surface recoil is partly a consequence of the lower translational energies required for rotational excitation; the threshold is only 75 meV compared to ~0.65 eV for dissociation on a static surface. Focusing on the CWV results for the rotational transition, we have the rather surprising finding that the CWV gives almost identical transition probabilities with either first or second order coupling, and moreover, both results follow very faithfully the exact solution! So the linear coupling approximation is quite sufficient to describe the surface recoil accompanying molecular rotational transitions. These features are quite different from those found for dissociation (Figure 2). A comparative detailed analysis of the dynamics of molecules undergoing rotational excitation with the dynamics of those dissociating shows that they essentially probe different regions of the PES.[41,44] Molecules that dissociate must clearly pass around the elbow exploring the PES at extended bond lengths before reaching the products channel, whereas we find that for rotational excitation the majority of molecules traverse only the entrance channel region before significant bond extension has occurred. We shall show below that it is primarily this that determines the performance of the different levels of approximation in the CWV formalism.

4. Two-Dimensional Analysis Using Model PESs

The results from the high-dimensional computations show that for the same PES different levels of approximation to the surface motion are required for an accurate description of different processes. In this section, we shall show that the topography of the PES in the regions explored by the molecule is the key determinant. We have computed the dissociation probability for a reduced dimensional model PES with adjustable topography. Specifically, we omit the degrees-of-freedom relating to molecular orientation, leaving a two-dimensional model where only Z and r are retained for a bond angle $\theta = \pi/2$ (broadside orientation). Thus, we lose the capacity to treat rotational transitions but are still able to address dissociation and vibrational transitions. Figure 4 shows three PESs used, each of which has a dissociation barrier of the same height, 0.5 eV, but in a different location along the reaction path. PES (c) shown in Figure 4 is essentially the same as the

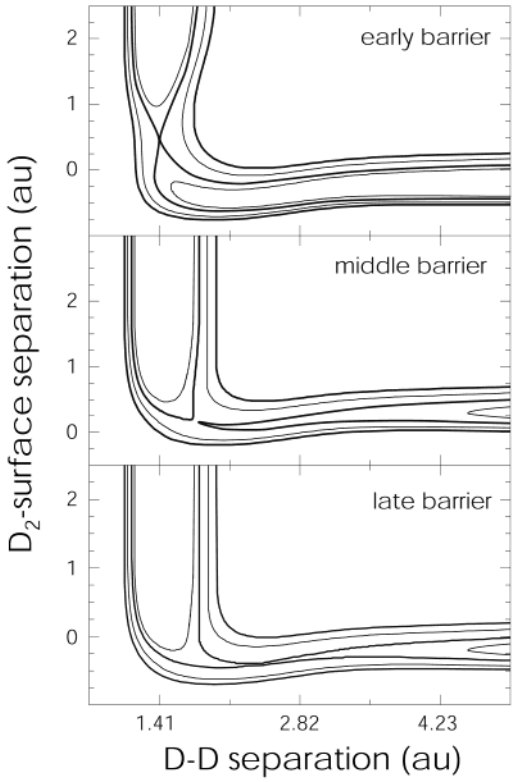

Figure 4. Two-dimensional model PESs used in the present study. In all cases shown, a dissociation barrier of 0.5 eV is present but with three different locations. In the entrance channel for PES (a), in the elbow for (b), and in the exit channel for (c).

D_2/Cu PES for the broad-side approach (Figure 1), except that the barrier height is reduced. This is a "late" barrier in the sense that its location is closer to the exit channel rather than the entrance channel. PESs (a) and (b) are variants of PES (c). The barrier height is maintained, but the location is shifted to the entrance channel for PES (a) ("early" barrier) or to an intermediate location for PES (b) ("middle" barrier).

The results of the dynamics calculations for the dissociation probability of ($v = 0$) D_2 on these PESs are shown in Figure 5. In the case of the late barrier, one observes the same surface recoil and discrepancies between first-order CWV results and the exact WP solution as discussed above for the higher-dimensionality calculations for dissociation (Figure 2). Also similar to Figure 2, the result obtained with second order coupling (not shown in Figure 5) shows a marked improvement, being almost identical to the exact solution. Turning to the results for the middle barrier and for the early barrier, we see that the magnitude of the recoil is relatively constant; however, the performance of the first order approximation changes dramatically. In the case of the early barrier, the CWV probability is very close to the exact result. This is particularly true in the tunneling regime, suggesting a good description of energy transfer by the linear coupling approximation. The result for the middle barrier shows a performance intermediate between the early and late barrier PESs.

The dependence of the accuracy of a particular level of the perturbative expansion of the molecule−phonon coupling on the topography of the PES can be understood by considering the form of the coupling $V^{(1)}$. This is just the first derivative of the PES with respect to Z. For an early barrier, the barrier is a maximum in the Z-direction giving an overall repulsive contribution resulting in the recoil effect in the dissociation. However, when the barrier is late, located round the elbow in

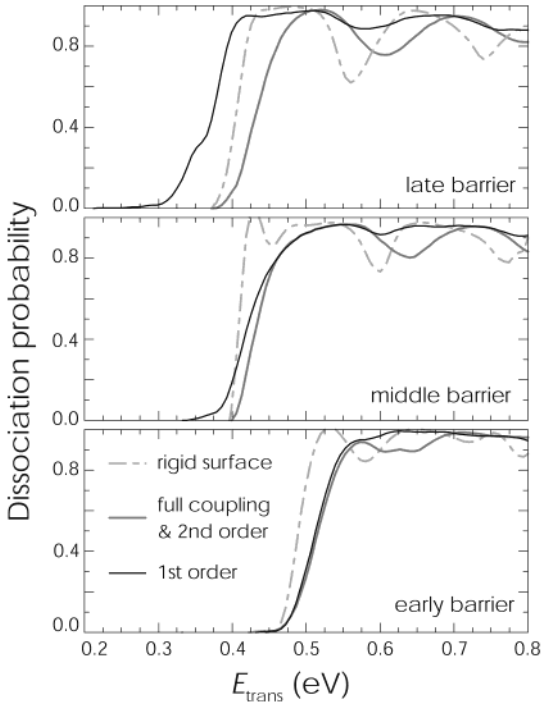

Figure 5. Probability for D_2 dissociation versus translational energy from the two-dimensional calculations using the model PESs shown in Figure 4. For each PES, the results of direct wave packet propagation are shown for a static surface (light gray dot−dashed lines) and for a surface at 0 K including recoil (solid gray lines). The results of these latter sets of calculations are identical with the second order 0 K calculations using the coupled wave vector method. The results of the linear coupling calculations using this method are shown as solid black lines.

the products channel, it is at a minimum in *Z*. In the reactants (gas-phase) region of this PES, the phonon contribution is still repulsive, and so we see an overall surface recoil when only this part of the PES is accessed, as we saw above for the rotational excitation. At the barrier maximum, the coupling term is now attractive, and the barrier height is effectively reduced. Therefore, if only the first order term in the phonon coupling is retained, there is effectively a lower dissociation barrier, and the threshold is actually downshifted relative to the static surface result, as can be seen in Figure 5. This discrepancy is remedied by inclusion of the second-order coupling term.

5. Conclusions

In summary, we have extended a coupled wave vector (CWV) formalism to high-dimensionality to describe a diatomic molecule dissociating on and scattering from a moving metal surface. Under the widely used single surface oscillator approximation, the CWV method provides a solution to the reduced density matrix for the molecule−heat-bath system and is less demanding computationally compared to the density matrix formalism and the direct Boltzmann averaging based on wave packet propagation in current use. This advantage of the CWV method is particularly meaningful for realistic, high-dimensional dynamics studies, and the computational saving is maximal if the Hamiltonian can be truncated to first-order (linear) terms or second-order (quadratic) terms in the molecule−phonon coupling. A central issue is then whether these lowest levels of approximation are sufficient or not.

Using a well-defined phenomenon, the lattice recoil at low surface temperature, we have addressed the issue of the accuracy of the truncated phonon expansion, focusing on an activated system, D_2/Cu(111), as an example. It has been found that at zero surface temperature the linear coupling approximation provides an adequate description of rotationally inelastic scattering between low-lying levels, but it fails seriously for dissociation. Inclusion of the quadratic coupling terms virtually eliminates the discrepancy giving results almost identical to the exact ones. Both processes studied serve as two extremes: the scattering process is characterized by low energy threshold with molecules exploring only the entrance channel (gas-phase side) of the PES, whereas in dissociation, the molecules energetically interacts with the PES traversing the whole of the elbow to reach the exit (products) channel.

The role of PES topology in determining the performance of the approximations has been revealed in detail in a two-dimensional analysis carried out in the present study. Dynamics calculations have been done on three PESs, which have similar activation energies but differing locations for the barrier. It has been found that the inadequacy of the linear coupling approximation for D_2 dissociation can be attributed to a "late" dissociation barrier, located in the exit or products channel. For the PES with the barrier located in the entrance channel (early barrier), the linear coupling approximation turns out to be adequate to describe dissociation dynamics, whereas a medium performance of this approximation occurs for the PES with the barrier between the entrance and exit channels.

These findings should apply generally for activated systems and serve as guidelines for performing the CWV computation using realistic, high-dimensional PESs. If the linear (quadratic) coupling approximation is valid, tremendous saving in computation can be achieved because one then needs to deal with only a small group of nonzero couplings.

Acknowledgment. This work was supported in part by the EPSRC (Ref. No. GR/L98480). B.J. acknowledges support from the National Science Foundation under Grant No. CHE-9877007.

References and Notes

(1) *Dynamics of gas−Surface Interactions*; Rettner, C. T., Ashfold, M. N. R., Eds.; Royal Society of Chemistry: London, 1991.
(2) Darling, G. R.; Holloway, S. *Rep. Prog. Phys.* **1995**, *58*, 1595.
(3) Gostein, M.; Parhikhteh, H.; Sitz, G. O. *Phys. Rev. Lett.* **1995**, *75*, 342.
(4) Hodgson, A.; Samson, P.; Wight, A.; Cottrell, C. *Phys. Rev. Lett.* **1997**, *78*, 963.
(5) Gillan, M. J. *Contemp. Phys.* **1997**, *38*, 115.
(6) Kroes, G. J. *Prog. Surf. Sci.* **1999**, *60*, 1.
(7) Wang, Z. S.; Darling, G. R.; Holloway, S. *Phys. Rev. Lett.* **2001**, *87*, 6102.
(8) Michelsen, H. A.; Rettner, C. T.; Auerbach, D. J. In *Surface Reactions*; Madix, R. J., Ed.; Springer: Berlin, 1993; p 123.
(9) Murphy, M. J.; Hodgson, A. *J. Chem. Phys.* **1998**, *108*, 4199.
(10) Gostein, M.; Watts, E.; Sitz, G. O. *Phys. Rev. Lett.* **1997**, *79*, 2891.
(11) Watts, E.; Sitz, G. O. *J. Chem. Phys.* **1999**, *111*, 9791.
(12) Watts, E.; Sitz, G. O. *J. Chem. Phys.* **2001**, *114*, 4171.
(13) Darling, G. R.; Kay, M.; Holloway, S. *Surf. Sci.* **1998**, *400*, 314.
(14) Gross, A.; Scheffler, M. *Phys. Rev.* **1998**, *B 57*, 2493.
(15) Busnengo, H. F.; Dong, W.; Salin, A. *Chem. Phys. Lett.* **2000**, *320*, 328.
(16) Busnengo, H. F.; Crespos, C.; Dong, W.; Salin, A.; Rayez, J. C. *Phys. Rev.* **2001**, *B 63*, 041402.
(17) Busnengo, H. F.; Dong, W.; Sautet, P.; Salin, A. *Phys. Rev. Lett.* **2001**, *87*, 7601.
(18) Crespos, C.; Busnengo, C.; Dong, W.; Salin, A. *J. Chem. Phys.* **2001**, *114*, 10954.
(19) Gross, A.; Wilke, S.; Scheffler, M. *Phys. Rev. Lett.* **1995**, *75*, 2718.
(20) Stiles, M. D.; Wilkins, J. W.; Persson, M. *Phys. Rev.* **1986**, *B 34*, 4490.
(21) Jackson, B. *J. Comput. Phys.* **1992**, *97*, 6792.
(22) Saalfrank, P.; Baer, R.; Kosloff, R. *Chem. Phys. Lett.* **1994**, *230*, 463.
(23) Pesce, L.; Saalfrank, P. *J. Chem. Phys.* **1998**, *108*, 3045.

(24) Jackson, B. *J. Chem. Phys.* **1998**, *108*, 1131.
(25) Logan, R. M.; Stickney, R. E. *J. Chem. Phys.* **1965**, *44*, 195.
(26) Logan, R. M.; Keck, J. C. *J. Chem. Phys.* **1968**, *49*, 860.
(27) Dino, W. A.; Kasai, H.; Okiji, A. *Prog. Surf. Sci.* **2000**, *63*, 63.
(28) Brenig, W.; Hilf, M. F. *J. Phys.: Condens. Matter* **2001**, *13*, R61.
(29) Luntz, A. C.; Harris, J. *Surf. Sci.* **1991**, *258*, 397.
(30) Jackson, B. *Chem. Phys. Lett.* **1999**, *308*, 456.
(31) Trail, J. R.; Graham, M. C.; Bird, D. M.; Persson, M.; Holloway, S. *Phys. Rev. Lett.* **2002**, *88*, 166802.
(32) Hand, M.; Harris, J. *J. Chem. Phys.* **1990**, *92*, 7610.
(33) Barker, J. A.; Auerbach, D. J. *Surf. Sci. Rep.* **1979**, *4*, 1.
(34) Doll, J. D.; Myers, L. E.; Adelman, S. A. *J. Chem. Phys.* **1975**, *63*, 4908.
(35) Hensel, M.; Korsch, H. J. *J. Phys.* **1992**, *A25*, 2043.
(36) Dohle, M.; Saalfrank, P. *Surf. Sci.* **1997**, *373*, 95.
(37) Feit, M. D.; Fleck, J. A., Jr.; Steiger, A. *J. Comput. Phys.* **1982**, *47*, 412.
(38) Darling, G. R.; Wang, Z. S.; Holloway, S. *Phys. Chem. Chem. Phys.* **2000**, *2*, 911.
(39) Tal-Ezer, H.; Kosloff, R. *J. Chem. Phys.* **1984**, *81*, 3967.
(40) Wang, Z. S.; Darling, G. R.; Holloway, S., Eds., 2002, in preparation.
(41) Wang, Z. S.; Darling, G. R.; Holloway, S. *Surf. Sci.* **2000**, *458*, 63.
(42) Kroes, G. J.; Wiesenekker, G.; Baerends, E. J.; Mowrey, R. C. *Phys. Rev.* **1996**, *B53*, 10397.
(43) Darling, G. R.; Holloway, S. *Surf. Sci.* **1994**, *321*, L189.
(44) Wang, Z. S.; Darling, G. R.; Holloway, S. *Surf. Sci.* **2002**, *504*, 66.